

That is, for $K = J^{-1}$

$$\begin{pmatrix} d \ln m \\ d \ln l \\ d \ln h \end{pmatrix} = K \begin{pmatrix} dM \\ dL \\ dH \end{pmatrix} \quad (\text{II})$$

A more general statement of eq 21 thus becomes

$$\left(\frac{\partial p X_i}{\partial \log \beta_j} \right)_{\beta_k \neq j} = - \sum_{i=1}^3 K_{ij} e_{ij} C_j \quad (26)$$

This simple relationship proves to be extremely useful and is a substantial shortcut in the least-squares refinement of equilibrium data.

Conclusion

The variation techniques presented by Osterberg,¹ Sarkar and Kruck,² and McBryde³ are powerful extensions of the pH titration experiment, particularly for equilibria involving polymeric species. We have presented a completely general mathematical basis for these techniques to multicomponent systems. Very useful relationships involving partial derivatives were used in the process. One of the relations derived allows for the first time the use of analytical derivatives in the refinement of equilibrium constants. However, the most important task remains the acquisition of data of sufficient accuracy so that these techniques can be successfully applied.¹⁸

Acknowledgment. This work was supported by the Division of Nuclear Sciences, Office of Basic Energy Sciences, U.S.

Department of Energy. We thank Mr. Vince Pecoraro and Dr. Wesley Harris for their helpful discussion and suggestions.

References and Notes

- (1) R. Osterberg, *Acta Chem. Scand.*, **14**, 471 (1960).
- (2) B. Sarkar and T. P. A. Kruck, *Can. J. Chem.*, **51**, 3541 (1973).
- (3) W. A. E. McBryde, *Can. J. Chem.*, **51**, 3572 (1973).
- (4) B. Hedström, *Acta Chem. Scand.*, **9**, 613 (1955).
- (5) L. G. Sillén, *Acta Chem. Scand.*, **15**, 1981 (1961).
- (6) T. P. A. Kruck and B. Sarkar, *Can. J. Chem.*, **51**, 3549 (1973).
- (7) T. P. A. Kruck and B. Sarkar, *Can. J. Chem.*, **51**, 3555 (1973).
- (8) S.-J. Lau, T. P. A. Kruck, and B. Sarkar, *J. Biol. Chem.*, **249**, 5878 (1974).
- (9) T. P. A. Kruck, S.-J. Lau, and B. Sarkar, *Can. J. Chem.*, **54**, 1300 (1976).
- (10) A. Avdeef, T. L. Bregante, and K. N. Raymond, paper in preparation.
- (11) A. Avdeef, paper in preparation.
- (12) (a) I. G. Sayce, *Talanta*, **15**, 1397 (1968); (b) A. Sabatini, A. Vacca, and P. Gans, *ibid.*, **21**, 53 (1974).
- (13) We assume Table II in ref 8 has a mislabeling with respect to the q values for the ligand constants. The order should be reversed.
- (14) The reported⁸ change in titrant volume at pH 6 is about 0.6 mL of 1.0024 M NaOH. We calculate a change of only 4 ligand equiv or only 0.029 mL. This inconsistency could be explained if the true titrant concentration were 0.05 M, rather than the reported value of 1.0024 M.
- (15) G. Gutnikov and H. Freiser, *Anal. Chem.*, **40**, 39 (1968).
- (16) H. Margenau and G. M. Murphy, "The Mathematics of Physics and Chemistry", Van Nostrand, New York, 1943, pp 17-21.
- (17) The data $(H, L)_{\text{pH}}$ or $(H, M)_{\text{pH}}$ can be obtained from a series of titration curves, such as in Figures 1 to 3, in the following manner: One can overlay the curves with a uniformly spaced series of horizontal lines of constant pH. Each line intersects the titration curves of different values of L or M . The corresponding titrant values, EQV, at the points of intersection are readily converted to values of H .
- (18) T. B. Field and W. A. E. McBryde, *J. Can. Chem.*, **56**, 1202 (1978). These authors also considered the variation method with computer-generated data and presented an excellent critical evaluation of data handling.

Contribution from the Department of Chemistry,
University of California, Berkeley, California 94720

Crystal and Molecular Structures of Tetrakis(catecholato)hafnate(IV) and -cerate(IV). Further Evidence for a Ligand Field Effect in the Structure of Tetrakis(catecholato)uranate(IV)

STEPHEN R. SOFEN, STEPHEN R. COOPER, and KENNETH N. RAYMOND*

Received October 31, 1978

Crystals of the isostructural title compounds, $\text{Na}_4[\text{M}(\text{O}_2\text{C}_6\text{H}_4)_4] \cdot 21\text{H}_2\text{O}$ ($\text{M} = \text{Hf}, \text{Ce}$), have been obtained from basic aqueous solutions and examined by X-ray diffraction, by using counter data. Previously a small structural distortion of the analogous uranium complex was observed which leads to a difference in metal-oxygen bond lengths of the A and B sites of the coordination polyhedron (trigonal-faced dodecahedron, D_{2d} molecular symmetry) formed by the catechol ligands. The present results on the undistorted cerium complex, in conjunction with previous results on the thorium compound (which is also undistorted), eliminate explanations based on differences in metal ionic radius since that of U(IV) is between those of Th(IV) and Ce(IV). The results reported here thus support earlier suggestions that the distortion observed for the uranium complex is attributable to a small ligand field effect of the two 5f electrons of U(IV). Ionic radius considerations alone do not lead to structural distortion until $\text{M} = \text{Hf}$, which has the smallest ionic radius of the four metals examined. Examination of the remarkably stable cerium complex, which is deep red ($\lambda_{\text{max}} 517 \text{ nm}$; $\epsilon 2350$), has shown this complex to be diamagnetic, militating against a cerium(III)-(semiquinone)tris(catecholato) formulation and in favor of a cerium(IV)-tetrakis(catecholato) description. The Ce(IV) complex is found by cyclic voltammetry to undergo a quasi-reversible one-electron reduction (in strongly basic solution with excess catechol) with $E_f = -692 \text{ mV}$ vs. SCE. The observed formal potential of the $\text{Ce}^{\text{IV/III}}(\text{cat})_4$ couple, taken with the corresponding Ce(IV)/Ce(III) standard potential, implies that the tetrakis formation constants (i.e., K for $\text{M}^{n+} + 4\text{cat}^{2-} = [\text{M}(\text{cat})_4]^{n-8}$) for Ce(IV) and Ce(III) differ by a factor of 10^{36} . Both the colorless Hf and the red Ce complexes have 4 site symmetry in the space group $I4_1$, $Z = 2$ (with $a = 14.486$ (1) Å, $c = 9.984$ (1) Å for Hf; $a = 14.649$ (2) Å, $c = 9.976$ (1) Å for Ce). For Hf the 4549 independent data with $F_o^2 > 3\sigma(F_o^2)$ converged to unweighted and weighted R factors of 3.3 and 4.5%, respectively, upon full-matrix least-squares refinement with anisotropic thermal parameters for all nonhydrogen atoms. The corresponding R factors for the Ce complex are 4.3 and 5.3%, respectively, on the basis of 3106 independent data. Ring O-M-O angles of 71.5 (1)° for Hf and 68.3 (1)° for Ce are found, with M-O bond lengths of 2.194 (3) and 2.220 (3) Å for Hf, compared with 2.357 (4) and 2.362 (4) Å for Ce.

Introduction

Although the presence of ligand field effects has been suggested for actinide complexes, definitive recognition of such effects has been hampered by the complex interplay of 5f, 6d, and 7s orbitals for the actinides and the lack of a suitable

isostructural series to preclude changes in crystal packing forces.

Previous investigations for actinide-specific chelators analogous to microbial iron transport chelates led us to examine the structures of the tetrakis(catecholato) complexes

of U(IV) and Th(IV), in which a small structural distortion was observed for the uranium complex.¹ This distortion renders the two catechol oxygens of a given molecule inequivalent, in contrast to the thorium case, and was tentatively attributed to the presence of a ligand field effect induced by the two 5f electrons of U(IV). However, the importance of another possible cause of this distortion, the smaller ionic radius of uranium(IV) vs. thorium(IV), could not be evaluated. As an extension of our previous interest in catechol coordination chemistry and for clarification of the structural effect of the 5f electrons the corresponding Hf complex was prepared and examined crystallographically. The results of this structure were—by themselves—ambiguous as far as the metal–oxygen bond distance distortion problem mentioned above.

In the course of this work, it became apparent that, somewhat surprisingly, the analogous Ce(IV) chelate could be prepared, surprising because the strongly oxidizing Ce(IV) ion ($E_0 = +1.70$ V²) might have been expected to react with a facile reducing agent such as the catechol dianion.³ That the cerium complex exists is a reflection of the impressive coordinating ability of the catechol group, which coordinates and stabilizes with respect to reduction such oxidizing ions as Fe(III),⁴ V(V),⁵ and Mn(III).⁶ In an effort to understand the distortions of the dodecahedral skeleton observed for the [U(cat)₄]⁴⁻ complex, we have prepared and characterized structurally the analogous hafnium(IV) and cerium(IV) complexes and examined the optical, magnetic, and electrochemical properties of the cerium chelate; the results are reported here.

Experimental Section

Both Na₄[M(O₂C₆H₄)₄]·21H₂O (M = Ce, Hf) complexes were prepared by using the methods and precautions described in the synthesis of the thorium and uranium complexes¹ with anhydrous hafnium tetrachloride and ceric ammonium nitrate as the metal starting materials. As before, crystals suitable for X-ray diffraction were obtained by slow cooling of the filtrate of the reaction mixture. X-ray precession photographs verified that the compounds were the desired isostructural analogues to the thorium and uranium compounds.

Infrared spectra were obtained on a Perkin-Elmer 283 spectrometer as KBr pellets. Solutions for optical studies of [Ce(cat)₄]⁴⁻ were prepared by pipetting an aqueous stock solution of recrystallized⁷ (NH₄)₂Ce(NO₃)₆ into an N₂-purged solution of catechol ([cat]/[Ce] = 18) in 1 M NaOH, and the spectra were recorded on a Cary 118 spectrometer. Cyclic voltammetry was performed in 5 M NaOH solutions which were 1 M in catechol by using hanging mercury drop electrodes; preparative reductions were performed on stirred mercury pool electrodes, in both cases by employing previously described equipment.⁸ Magnetic measurements were conducted on a Princeton Applied Research Model 155 vibrating sample magnetometer, as previously described.¹

Unit Cell and Diffraction Data. The efflorescent crystals were mounted in 0.3 mm (Hf) or 0.2 mm (Ce) quartz capillaries under water-saturated, oxygen-free nitrogen in a glovebag. The cerium crystal was mounted with the long edge approximately coincident with the diffractometer ϕ axis. The crystals were oriented on the CAD-4 diffractometer using the automatic search and centering routines of the Enraf-Nonius computing package. Previous work¹ had shown that this class of compounds crystallizes in the body-centered tetragonal space group $I4$. Crystal data obtained by a least-squares fit to 25 high-angle reflections are in Table I.

Intensity data were collected on a Nonius CAD-4 automated diffractometer using monochromatic Mo K α radiation.⁹⁻¹¹ The data were processed as previously described with parameter p , introduced to prevent overweighting strong reflections, chosen as 0.04.¹² The complicated morphology of the Hf data crystal necessitated calculation and application of a spherical absorption correction. No absorption correction was calculated for the cerium salt since it was impossible to index all of the faces because of grease and since ψ scans revealed a maximum difference in transmission of 10% for several test reflections. Crystal densities for the Hf and Ce complexes (1.69 (1) and 1.64 (1) g/cm³, respectively; 1.71 and 1.65 g/cm³ calculated for

Table I. Summary of Crystal Data for Na₄[M(O₂C₆H₄)₄]·21H₂O, M = Hf, Ce

complex	Hf	Ce
mol wt	1081.3	1042.9
space group	$I4$	$I4$
cell constants ^a		
<i>a</i> , Å	14.486 (1)	14.649 (2)
<i>c</i> , Å	9.984 (1)	9.976 (1)
cell volume, Å ³	2095.1	2140.8
formula units/cell	2	2
calcd density	1.71	1.65
obsd density	1.69 (1)	1.64 (1)
$\mu_{\text{MoK}\alpha}$, cm ⁻¹	26.0	12.1
crystal shape	approx sphere, radius = 0.14 mm	approx parallelepiped, 0.20 × 0.18 × 0.28 mm

^a Ambient temperature of 26 °C; Mo K α radiation, λ 0.709 30 Å.

$Z = 2$) were determined by flotation in dibromomethane–heptane mixtures.

Solution and Refinement of the Structures. As precession photographs revealed that the unit cell of the Hf complex is nearly identical with those of the Th and U complexes, the structure solution began with the final positional parameters from the latter. After three cycles of full-matrix least-squares refinement (using anisotropic thermal parameters for all nonhydrogen atoms) with 4549 independent reflections having $F_o^2 > 3\sigma(F_o^2)$ the weighted (R_w) and unweighted (R) agreement factors were 4.6 and 3.4%, respectively.¹³⁻¹⁷ At this point the four ligand H atoms were entered as fixed atoms (with isotropic temperature factors of 5.0 Å²) at positions calculated by assuming a C–H bond distance of 0.95 Å.¹⁸ None of the water hydrogens were located. The final agreement factors are $R = 3.3\%$ and $R_w = 4.5\%$ and the error in an observation of unit weight is 1.5.

The structure solution of the cerium complex was like that of the hafnium analogue. Full-matrix least-squares refinement of 3106 unique reflections with $F_o^2 > 3\sigma(F_o^2)$ converged to unweighted (R) and weighted (R_w) agreement factors of 4.3 and 6.3%, respectively.¹⁷ Positional and thermal parameters for the nonhydrogen atoms of the Hf and Ce structures are summarized in Tables II and V, respectively, while Table IV lists the amplitudes of vibration for the structures, which were derived from the thermal parameters.¹⁹ Final positional parameters for the fixed hydrogen atoms were calculated as described above (no water hydrogens were found) and the results for both Ce and Hf collected in Table III.

Results

Description of the Structures. As for the thorium and uranium complexes, the crystal structure consists of discrete, eight-coordinate [M(cat)₄]⁴⁻ dodecahedra, sodium ions, and waters of crystallization (Figures 1–3). The 21 waters form a hydrogen-bonded network throughout the crystal, with the sodium ion coordinated to two catecholate oxygens and four water oxygens.

Bond lengths and angles for both complexes are shown in Figure 4 and are listed in Tables VI and VII. Average M–O bond lengths are 2.360 (4) Å for Ce and 2.207 (3) Å for Hf, with corresponding O–M–O angles of 68.3 (1) and 71.5 (1)°. By comparison with the present structure, average Hf^{IV}–O bond lengths of 2.19 (1) and 2.382 (10) Å are found for the tetrakis(oxalato)²⁰ and -(tropolonato)²¹ complexes, while average Ce^{IV}–O distances are 2.32 (4) Å for tetrakis(acetylacetonato)cerate(IV)²² and 2.56 Å for cerium(IV) acetate.²³

Physical Studies. In contrast to the colorless Hf complex, the analogous cerium catecholate is a deep red, with a band maximum at 517 nm (ϵ 2350) (Figure 5). Cyclic voltammetric examination of the [Ce(cat)₄]⁴⁻ complex in strongly basic solution containing excess catechol revealed a quasi-reversible, one-electron wave with formal potential $E_f = -692$ mV vs. saturated calomel electrode (SCE) and peak potential separation of 72 mV (Figure 6). Upon preparative reduction at a stirred mercury pool, the red Ce(IV) complex is quantitatively and reversibly reduced to the colorless Ce(III) complex, consuming one electron per Ce(IV). Magnetic

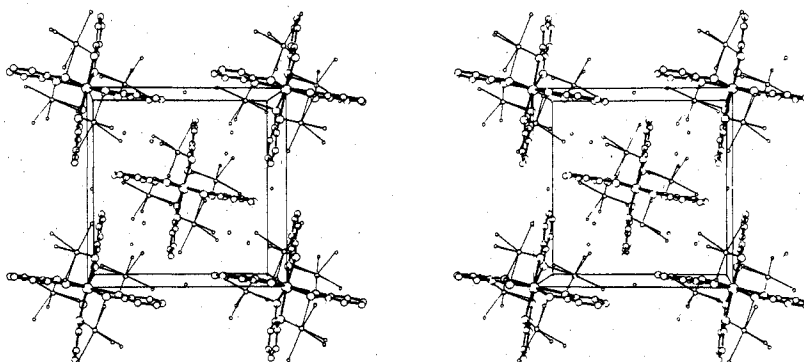


Figure 1. A stereoscopic packing diagram of the $\text{Na}_4[\text{M}(\text{O}_2\text{C}_6\text{H}_4)_4] \cdot 21\text{H}_2\text{O}$ ($\text{M} = \text{Hf}, \text{Ce}$) structures viewed down the crystallographic c axis.

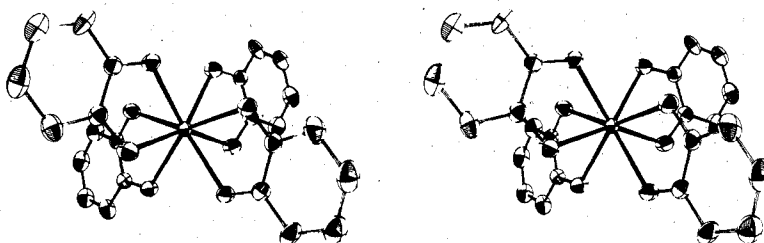


Figure 2. A stereoscopic ORTEP drawing of the $[\text{M}(\text{O}_2\text{C}_6\text{H}_4)_4]^{4+}$ ($\text{M} = \text{Hf}, \text{Ce}$) unit viewed down the molecular twofold axis. The $\bar{4}$ axis is vertical. The individual atoms are drawn at 50% probability contours of the thermal motion in the Ce structure.

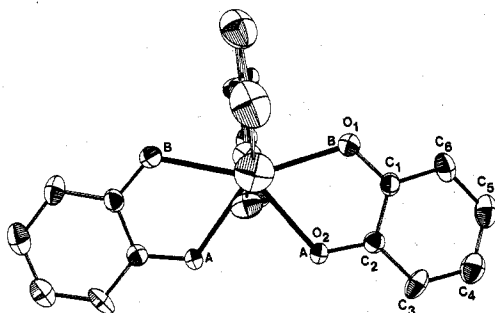


Figure 3. The $[\text{M}(\text{O}_2\text{C}_6\text{H}_4)_4]^{4-}$ anion viewed along the molecular mirror plane with the $\bar{4}$ axis vertical. The atom labels used in the text as well as the dodecahedral A and B sites are shown.

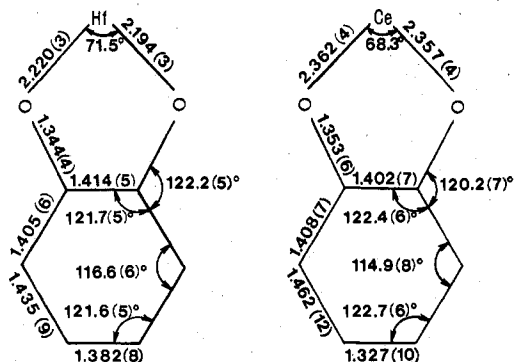


Figure 4. Schematic diagram of the hafnium(IV) and cerium(IV) catecholate coordination geometries, showing the average bond distances (\AA) and angles.

susceptibility measurements established that the Ce(IV) chelate is diamagnetic over the temperature range 4–300 K.

Discussion

Although a coordinated semiquinone formulation (with three catecholates) could not have been excluded a priori, the Ce complex is best considered as a simple cerium(IV) catechol complex. The diamagnetism of the Ce(IV) complex agrees with the crystallographic assignment of a simple catecholato formulation to this complex, rather than a semiquinone

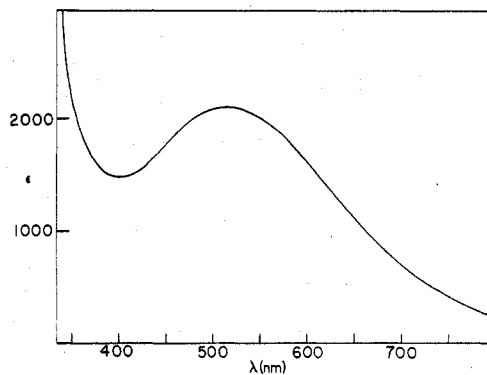


Figure 5. Absorption spectrum of $[\text{Ce}(\text{O}_2\text{C}_6\text{H}_4)_4]^{4-}$ in 1 M NaOH solution containing excess catechol.

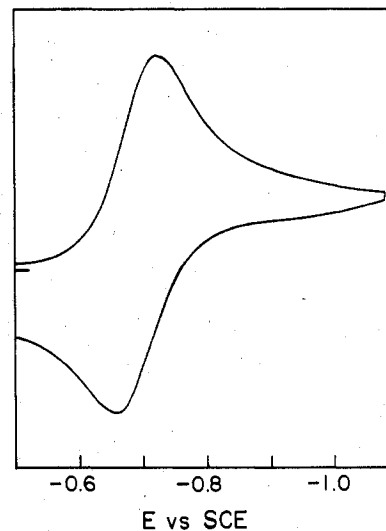


Figure 6. Cyclic voltammogram of $[\text{Ce}(\text{O}_2\text{C}_6\text{H}_4)_4]^{4-}$ in 5 M NaOH, 1 M catechol aqueous solution, on a hanging mercury drop electrode, at 100 mV/s scan rate.

formulation. If the Ce complex existed as the cerium(III) semiquinone, the weak coupling expected between the Ce(III)

Table II. Positional and Thermal Parameters ($\times 10^4$) for the Nonhydrogen Atoms in $\text{Na}_4[\text{Hf}(\text{O}_2\text{C}_6\text{H}_4)_4]\cdot 2\text{H}_2\text{O}$

atom	x	y	z	β_{11}^a	β_{22}	β_{33}	β_{12}	β_{13}	β_{23}
Hf ^b	0	0	0	18.83 (7) ^c	18.83 (7)	37.76 (17)	0	0	0
Na	0.18349 (15)	0.04341 (15)	0.7414 (2)	42.3 (9)	40.4 (9)	72.7 (16)	-3.7 (7)	5.0 (10)	6.8 (10)
O ₁	0.0379 (2)	0.14006 (19)	0.0630 (3)	36.9 (13)	24.5 (11)	47 (2)	-4.6 (9)	1.9 (13)	-0.7 (12)
O ₂	0.0237 (2)	0.08490 (17)	0.8181 (2)	35.7 (12)	19.8 (9)	46.5 (19)	-2.7 (8)	-1.1 (12)	1.4 (11)
O ₃ ^d	0.0592 (3)	0.0938 (4)	0.6094 (4)	56 (2)	64 (2)	89 (4)	-0.2 (19)	3 (2)	23 (3)
O ₄	0.3267 (3)	0.9710 (4)	0.6374 (5)	50 (2)	61 (2)	122 (5)	7.4 (18)	-4 (3)	-8 (3)
O ₅	0.2216 (3)	0.1321 (4)	0.5436 (5)	46 (2)	75 (3)	111 (4)	-8.5 (19)	-6 (2)	23 (3)
O ₆	0.2733 (4)	0.1676 (3)	0.8540 (5)	54 (2)	53 (2)	121 (5)	-6.1 (19)	2 (3)	-8 (3)
O ₇	0.2814 (3)	0.3184 (3)	0.6484 (5)	44 (2)	34.9 (17)	161 (6)	-1.2 (15)	17 (3)	-9 (2)
O ₈ ^e	0	1/2	1/4	45 (3)	45 (3)	206 (16)	0	0	0
C ₁	0.0433 (2)	0.2066 (2)	0.9686 (3)	25.9 (13)	23.6 (12)	57 (3)	-2.9 (10)	0.2 (13)	0.2 (12)
C ₂	0.0369 (2)	0.1756 (2)	0.8347 (3)	21.8 (12)	20.4 (12)	58 (3)	0.5 (9)	1.7 (14)	3.3 (14)
C ₃	0.0470 (3)	0.2393 (3)	0.7302 (4)	29.9 (15)	32.1 (16)	66 (3)	-1.2 (12)	-4.8 (18)	15.9 (18)
C ₄	0.0610 (3)	0.3322 (3)	0.7594 (5)	34.3 (18)	29.6 (17)	101 (5)	-2.7 (14)	-8 (2)	21 (2)
C ₅	0.0640 (4)	0.3628 (3)	0.8904 (6)	44 (2)	24.4 (16)	114 (5)	-3.7 (15)	-9 (3)	8 (2)
C ₆	0.0549 (3)	0.2297 (2)	0.0060 (12)	44.0 (15)	24.5 (11)	79 (4)	-6.3 (10)	-2 (5)	4 (4)

^a The form of the anisotropic thermal ellipsoid is $\exp[-(\beta_{11}h^2 + \beta_{22}k^2 + \beta_{33}l^2 + 2\beta_{12}hk + 2\beta_{13}hl + 2\beta_{23}kl)]$. ^b Located on the crystallographic 4 axis at 0, 0, 0. ^c Standard deviations of the least significant figures are given here and elsewhere in parentheses. ^d Atoms O₃-O₈ are water oxygens. ^e Located on the crystallographic 4 axis.

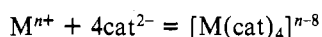
Table III. Positional Parameters for the Fixed Hydrogen Atoms^a

atom	x		y		z	
	Hf	Ce	Hf	Ce	Hf	Ce
H ₃	0.0442	0.0510	0.2192	0.2254	0.6398	0.6361
H ₄	0.0686	0.0765	0.3752	0.3794	0.6883	0.6852
H ₅	0.0723	0.0760	0.4269	0.4312	0.9069	0.8963
H ₆	0.0567	0.0574	0.3199	0.3266	0.0965	0.0950

^a The subscript of each hydrogen atom is chosen to be the same as the carbon to which it is bonded. The isotropic temperature factor for all the hydrogen atoms is 5.0 \AA^2 .

4f electron and the π electron of the ligand would be expected to yield an at least weakly paramagnetic complex.

The ratio of the formation constants of the cerium(IV) and -(III) tetrakis(catecholato) complexes, i.e., the equilibrium constants K_n for the reaction



can be calculated from the cyclic voltammetric data. The observed formal potential E_f of the $\text{Ce}^{\text{IV/III}}(\text{cat})_4$ couple (-692 mV vs. SCE; -448 mV vs. NHE) and the $\text{Ce}(\text{IV})/\text{Ce}(\text{III})$ standard potential ($E_0 = +1.70 \text{ V}$ vs. NHE²) are related by²⁴

$$E_f - E_0 = \frac{-59}{n} \log \frac{K_{\text{IV}}}{K_{\text{III}}} \text{ mV}$$

From these potentials the formation constants of the tetrakis

Table V. Positional and Thermal Parameters ($\times 10^4$) for the Nonhydrogen Atoms in $\text{Na}_4[\text{Ce}(\text{O}_2\text{C}_6\text{H}_4)_4]\cdot 2\text{H}_2\text{O}$

atom	x	y	z	β_{11}^a	β_{22}	β_{33}	β_{12}	β_{13}	β_{23}
Ce ^b	0	0	0	29.69 (13) ^c	20.69 (13)	45.6 (4)	0	0	0
Na	0.18562 (18)	0.04165 (18)	0.7387 (3)	46.6 (12)	43.9 (11)	84 (2)	-4.9 (9)	5.3 (14)	7.5 (13)
O ₁	0.0389 (3)	0.1504 (2)	0.0616 (4)	44.3 (18)	27.8 (16)	60 (3)	-6.7 (13)	6 (2)	-1.3 (17)
O ₂	0.0276 (3)	0.0926 (2)	0.8105 (4)	41.4 (17)	23.1 (13)	62 (3)	-0.9 (12)	-2.6 (18)	-0.7 (16)
O ₃ ^d	0.0606 (4)	0.0945 (5)	0.6113 (6)	63 (3)	77 (4)	112 (6)	-3 (3)	-1 (3)	35 (4)
O ₄	0.3267 (4)	0.9693 (4)	0.6373 (7)	54 (3)	65 (3)	141 (7)	7 (2)	-5 (4)	-7 (4)
O ₅	0.2223 (4)	0.1318 (5)	0.5420 (6)	48 (2)	85 (4)	110 (6)	-6 (2)	-5 (3)	18 (3)
O ₆	0.2725 (5)	0.1667 (4)	0.8512 (7)	60 (3)	58 (3)	139 (7)	-3 (2)	2 (4)	-11 (4)
O ₇	0.2830 (4)	0.3174 (4)	0.6465 (7)	44 (2)	44 (2)	170 (8)	-0.3 (19)	14 (4)	-11 (3)
O ₈ ^e	0	1/2	1/4	47 (3)	47 (3)	215 (21)	0	0	0
C ₁	0.0451 (3)	0.2138 (3)	0.9638 (5)	28.7 (17)	24.9 (18)	78 (5)	-3.6 (13)	1.0 (19)	0 (19)
C ₂	0.0408 (3)	0.1831 (3)	0.8308 (5)	25.0 (16)	23.7 (16)	64 (4)	0 (13)	2 (2)	6 (2)
C ₃	0.0526 (4)	0.2454 (4)	0.7267 (6)	34 (2)	37 (2)	83 (5)	0.7 (17)	-4 (3)	21 (3)
C ₄	0.0671 (4)	0.3374 (4)	0.7565 (7)	34 (2)	38 (2)	121 (7)	-2.1 (18)	-8 (3)	29 (3)
C ₅	0.0679 (5)	0.3676 (4)	0.8819 (7)	48 (3)	25 (2)	128 (8)	-5.3 (19)	-14 (4)	7 (3)
C ₆	0.0567 (4)	0.3061 (3)	0.0044 (17)	47 (2)	26.2 (16)	130 (7)	-6.4 (14)	15 (8)	-7 (7)

^a The form of the anisotropic thermal ellipsoid is $\exp[-(\beta_{11}h^2 + \beta_{22}k^2 + \beta_{33}l^2 + 2\beta_{12}hk + 2\beta_{13}hl + 2\beta_{23}kl)]$. ^b Located on the crystallographic 4 axis at 0, 0, 0. ^c Standard deviations of the least significant figures are given here and elsewhere in parentheses. ^d Atoms O₃-O₈ are water oxygens. ^e Located on the crystallographic 4 axis.

complexes differ by a factor of 10^{36} . The relatively low value for K_{III} is consistent with the high base and catechol concentrations necessary to observe a reversible Ce(IV) to Ce(III) reduction without loss of a catechol ligand (and attendant irreversibility). Upon preparative electrochemical reduction to the cerous state, the intense charge-transfer band of the Ce(IV) chelate is reversibly lost, consistent with simple reduction of the complex.

The dodecahedral shape parameters for these complexes are given in Table VIII.²⁵ The experimentally determined differences in metal-oxygen distances for tetrakis(catecholato) complexes of hafnium, cerium, uranium, and thorium are given in Table IX for the A and B sites of the Hoard and Silverton dodecahedron.²⁶ As seen in Table IX, despite a significant difference in metal ionic radius, the metal-oxygen distances in the f⁰ cerium and thorium structures are equal within experimental error. Since the ionic radius of uranium lies between those of cerium and thorium, it is unlikely that the metal size has any great effect on the structure. We stress that all four of these complexes have identical unit cell contents and are identical except for the metal ion and conclude that the distortion of the uranium structure by lengthening of the M-O_A bond is attributable solely to the previously proposed¹ ligand field effect from the f electrons.

There remains the question of why the d⁰ hafnium complex shows a distortion equal to that found in the uranium complex. The ionic radius of hafnium is 0.22 Å smaller than that of thorium.²⁷ With such a small metal ion the catecholato ligands

Table VI. Bond Distances in $\text{Na}_4[\text{M}(\text{O}_2\text{C}_6\text{H}_4)_4] \cdot 21\text{H}_2\text{O}$, $\text{M} = \text{Hf, Ce}$

atoms	distance, Å		atoms	distance, Å	
	Hf	Ce		Hf	Ce
M-O ₁	2.194 (3)	2.357 (4)	Na-O ₃	2.348 (5)	2.360 (7)
M-O ₂	2.220 (3)	2.362 (4)	Na-O ₄	2.546 (5)	2.534 (7)
O ₁ -C ₁	1.350 (4)	1.350 (6)	Na-O ₅	2.419 (5)	2.427 (6)
O ₂ -C ₂	1.338 (4)	1.355 (5)	Na-O ₆	2.488 (5)	2.497 (7)
C ₁ -C ₂	1.414 (5)	1.402 (7)	O ₂ -O ₃	2.150 (5)	2.046 (7)
C ₂ -C ₃	1.400 (5)	1.394 (6)	O ₃ -O ₄	3.153 (9)	3.216 (13)
C ₃ -C ₄	1.392 (6)	1.396 (9)	O ₃ -O ₅	2.505 (6)	2.528 (8)
C ₄ -C ₅	1.382 (8)	1.327 (10)	O ₄ -O ₅	2.940 (7)	2.985 (9)
C ₅ -C ₆	1.478 (11)	1.527 (16)	O ₄ -O ₆	2.783 (5)	2.812 (6)
C ₆ -C ₁	1.410 (6)	1.422 (7)	O ₅ -O ₆	3.229 (7)	3.212 (9)
Na-O ₁	2.366 (3)	2.372 (5)	O ₅ -O ₇	3.021 (7)	3.045 (9)
Na-O ₂	2.512 (4)	2.535 (5)	O ₆ -O ₇	3.000 (7)	3.011 (9)

Table VII. Bond Angles in $\text{Na}_4[\text{M}(\text{O}_2\text{C}_6\text{H}_4)_4] \cdot 21\text{H}_2\text{O}$, $\text{M} = \text{Hf, Ce}$

atoms	angle, deg		atoms	angle, deg	
	Hf	Ce		Hf	Ce
O ₁ -M-O ₂	71.5 (1)	68.3 (1)	O ₁ -C ₁ -C ₂	115.4 (3)	117.4 (4)
O ₁ -M-O ₂ (90°) ^a	76.7 (1)	79.2 (1)	O ₁ -C ₁ -C ₆	120.4 (6)	117.2 (8)
O ₁ -M-O ₂ (180°)	141.8 (1)	141.9 (1)	O ₂ -C ₂ -C ₁	116.0 (3)	117.5 (4)
O ₁ -M-O ₁ (90°)	94.7 (4)	93.90 (5)	O ₂ -C ₂ -C ₃	124.8 (3)	123.1 (5)
O ₁ -M-O ₁ (180°)	146.7 (1)	149.8 (2)	C ₁ -C ₂ -C ₃	119.2 (3)	119.4 (4)
O ₂ -M-O ₂ (90°)	132.0 (1)	129.8 (1)	C ₂ -C ₃ -C ₄	119.8 (4)	119.5 (6)
O ₂ -M-O ₂ (180°)	70.2 (1)	73.7 (2)	C ₃ -C ₄ -C ₅	120.8 (4)	121.6 (5)
			C ₄ -C ₅ -C ₆	122.5 (5)	123.8 (6)
			C ₅ -C ₆ -C ₁	113.3 (8)	110.3 (11)
			C ₆ -C ₁ -C ₂	124.2 (6)	125.4 (8)

^a The angle between catechols containing the two oxygens is given in parentheses.

Table VIII. Shape Parameters (deg) for $[\text{M}(\text{O}_2\text{C}_6\text{H}_4)_4]^{4-}$ ($\text{M} = \text{Hf, Ce, U, Th}$)

	ϕ_1	ϕ_2	δ_1	δ_2	δ_3	δ_4	θ_A	θ_B
$[\text{Hf}(\text{O}_2\text{C}_6\text{H}_4)_4]^{4-}$	0.4	0.4	32.2	32.2	32.2	32.2	35.2	73.3
$[\text{Ce}(\text{O}_2\text{C}_6\text{H}_4)_4]^{4-}$	2.1	2.1	32.0	32.0	32.0	32.0	36.8	74.9
$[\text{U}(\text{O}_2\text{C}_6\text{H}_4)_4]^{4-}$	3.0	3.0	31.1	31.1	31.1	31.1	37.1	75.2
$[\text{Th}(\text{O}_2\text{C}_6\text{H}_4)_4]^{4-}$	3.6	3.6	31.3	31.3	31.3	31.3	37.9	75.4
D_{2d} dodecahedron ^a	0.0	0.0	29.5	29.5	29.5	29.5	35.2	73.5
D_{4d} square antiprism ^a	24.5	24.5	0.0	0.0	52.4	52.4	57.3	57.3

^a Shape parameters for the idealized geometries are from ref 25 and 26.

Table IX. Structural Parameters for $\text{Na}_4[\text{M}(\text{O}_2\text{C}_6\text{H}_4)_4] \cdot 21\text{H}_2\text{O}$ Complexes

metal	ionic radius, ^a Å	$[(\text{M}-\text{O}_A) - (\text{M}-\text{O}_B)]$, Å	O_A-O_A , Å
Hf	0.83	0.026 (4)	2.554 (5)
Ce	0.97	0.005 (5)	2.831 (7)
U	1.00	0.027 (5)	2.883 (7)
Th	1.05	0.004 (5)	2.972 (6)

^a Reference 27.

are pulled in sufficiently so that interligand contacts become significant. This is demonstrated in the last column of Table IX where the oxygen-oxygen distances between A sites related by the twofold axis are set out. For the hafnium complex this distance (2.550 Å) is nearly 0.3 Å less than for the cerium salt and is well within the van der Waals contact distance given by Pauling.²⁸ To avoid the energetically unfavorable interactions occasioned by further decrease in the O_A-O_A distance, the $\text{M}-\text{O}_A$ bond lengthens, yielding the observed distortion. Attempts at synthesis of the analogous Ti(IV) complex via the

procedure employed for the U, Th, Hf, and Ce chelates did not afford the tetrakis Ti(IV) complex, presumably because of these steric constraints.

In summary, the results reported here support the existence of small but significant ligand field effects from 5f electrons on molecular structure and establish that the unusual cerium(IV) tetrakis(catecholato) complex exists as such and not as tris(catecholato)(semiquinone).

Acknowledgment. We would like to thank Rodney Banks for a gift of purified HfCl_4 and Dr. Derek Freyberg for experimental assistance. The structural studies reported here are supported by the NSF.

Registry No. $\text{Na}_4[\text{Ce}(\text{O}_2\text{C}_6\text{H}_4)_4] \cdot 21\text{H}_2\text{O}$, 69847-05-8; $\text{Na}_4[\text{Hf}(\text{O}_2\text{C}_6\text{H}_4)_4] \cdot 21\text{H}_2\text{O}$, 69855-29-4.

Supplementary Material Available: A listing of structure factor amplitudes and Table IV showing root-mean-square amplitudes of vibration along principal axes (31 pages). Ordering information is given on any current masthead page.

References and Notes

- Sofen, S. R.; Abu-Dari, K.; Freyberg, D. P.; Raymond, K. N. *J. Am. Chem. Soc.* **1978**, *100*, 7882-7.
- Latimer, W. M. "Oxidation States of the Elements and Their Potentials in Aqueous Solution", 2nd ed.; Prentice-Hall: Englewood Cliffs, N.J., 1952; p 294.
- Ho, T.-L.; Hall, T. W.; Wong, C. M. *Chem. Ind. (London)* **1972**, 729-30.
- Raymond, K. N.; Isied, S. S.; Brown, L. D.; Fronczek, F. F.; Nibert, J. H. *J. Am. Chem. Soc.* **1976**, *98*, 1767-74.
- Cooper, S. R.; Freyberg, D. P.; Raymond, K. N., manuscript in preparation.
- Magers, K. D.; Smith, C. G.; Sawyer, D. T. *Inorg. Chem.* **1978**, *17*, 515-23.
- Vogel, A. I. "Quantitative Inorganic Analysis", 3rd ed.; Longman: London, 1961; pp 315-6.
- Cooper, S. R.; McArdle, J. V.; Raymond, K. N. *Proc. Natl. Acad. Sci. USA* **1978**, *75*, 3551-4.
- The programs used for the PDP 8/E computer were those written by Enraf-Nonius Corp. In addition to local programs for the Lawrence Berkeley Laboratory CDC 7600 computer, the following programs or modifications were used: Zalkin's FORDP Fourier program; Ibers' NUCLS, a group least-squares version of the Busing-Levy ORFLS program; ORFFE, a function and error program by Busing and Levy; Johnson's ORTEP, a thermal ellipsoid plot program.
- The θ - 2θ scan technique was used to collect intensity data for the unique form $h, k, \pm l$ to a 2θ angle of 60° for the cerium salt and to 70° for the hafnium salt. For the latter a duplicate form of $-h, k, \pm l$ was also collected and these data were averaged after correcting for absorption (R factor for averaging, 2.4% on F^2). For cerium, 700 low-angle duplicate reflections were collected before data acquisition was discontinued due to crystal decomposition (R factor for averaging, 2.5%). For each reflection the scan angle was extended 25% on each side to estimate the background count. The scan time was variable with a maximum of 90 s. During data collection on the hafnium compound the intensities of the 600, 060, and 004 reflections were measured as standards every 6000 s of X-ray exposure and showed no significant fluctuations. For the cerium compound, the 600, 060, and 004 reflections were monitored and showed a linear isotropic reduction of 2%. The data were corrected accordingly. For each crystal three high-angle orientation reflections were monitored every 200 reflections and a new orientation matrix was calculated if the setting angles had changed by more than 0.1° in any axis.
- An attenuator decreasing the intensity of the diffracted beam by a factor of 18.17 was automatically inserted into the beam when the prescan indicated an intensity too high for accurate counting. The θ scan angle was calculated as $(0.60 \pm 0.35 \tan \theta)$, and an aperture with a height of 4 mm and a variable width (width = $2.50 + 0.50 \tan \theta$) was located 173 mm from the crystal.
- Abu-Dari, K. I.; Ekstrand, J. D.; Freyberg, D. P.; Raymond, K. N. *Inorg. Chem.* **1979**, *18*, 108-12.
- In all refinements the function minimized was $\sum w(|F_o| - |F_c|)^2$, where F_o and F_c are the observed and calculated structure factors. The weighting factor w is $4F_c^2/\sigma^2(F_c^2)$. The atomic scattering factors for the nonhydrogen atoms were taken from the tabulations of Cromer and Mann.¹⁴ Hydrogen scattering factors were those calculated by Stewart, Davidson, and Simpson.¹⁵ Corrections for anomalous dispersion effects for the metal were made by using $\Delta f'$ and $\Delta f''$ values of Cromer.¹⁶
- Cromer, D. T.; Mann, B. *Acta Crystallogr., Sect. A* **1968**, *24*, 321-4.
- Stewart, R. F.; Davidson, E. R.; Simpson, W. T. *J. Chem. Phys.* **1965**, *42*, 3175-87.
- Cromer, D. T. *Acta Crystallogr.* **1965**, *18*, 17-23.
- $R = \sum ||F_o| - |F_c|| / \sum |F_o|$; $R_w = [\sum w(|F_o| - |F_c|)^2 / \sum w|F_o|^2]^{1/2}$. The error in an observation of unit weight is defined as $[\sum w(|F_o| - |F_c|)^2 / (N_{\text{obsd}} - N_{\text{var}})]^{1/2}$.
- Churchill, M. R. *Inorg. Chem.* **1973**, *12*, 1213-4.
- Supplementary material.

- (20) Tranqui, D.; Boyer, P.; Vulliet, P. *Acta Crystallogr., Sect. B* **1977**, *33*, 3126–33.
 (21) Tranqui, D.; Tissier, A.; Langier, J.; Boyer, P. *Acta Crystallogr., Sect. B* **1977**, *33*, 392–7.
 (22) Titze, H. *Acta Chem. Scand., Ser. A* **1974**, *28*, 1079–88.
 (23) Sadikov, G. G.; Kukina, G. A.; Porai-Koshits, M. A. *J. Struct. Chem. (Engl. Trans.)* **1971**, *12*, 787–92.
 (24) Meites, L. "Polarographic Techniques"; Wiley: New York, 1965; p 279.
 (25) Muetterties, E. L.; Guggenberger, L. J. *J. Am. Chem. Soc.* **1974**, *96*, 1748–56.
 (26) Hoard, J. L.; Silverton, J. V. *Inorg. Chem.* **1963**, *2*, 235–43.
 (27) Shannon, R. D. *Acta Crystallogr., Sect. A* **1976**, *32*, 751–67.
 (28) Pauling, L. "The Nature of the Chemical Bond", 3rd ed.; Cornell University Press: Ithaca, N.Y., 1960; p 260.

Contribution from the Department of Chemistry,
 University of Colorado, Boulder, Colorado 80309

Synthesis, Structure, and Properties of the Oxygen-Deficient Bis(3,5-di-*tert*-butylcatecholato)oxomolybdenum(VI) Dimer, $[\text{MoO}(\text{O}_2\text{C}_6\text{H}_2(t\text{-Bu})_2)_2]_2$

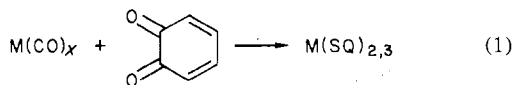
ROBERT M. BUCHANAN and CORTLANDT G. PIERPONT*

Received November 16, 1978

The reaction between $\text{Mo}(\text{CO})_6$ and 3,5-di-*tert*-butyl-1,2-benzoquinone in toluene produces a complex of empirical formula $\text{MoO}(\text{O}_2\text{C}_6\text{H}_2(t\text{-Bu})_2)_2$ as a toluene solvate. The results of a crystallographic molecular structure determination show that the complex is a centrosymmetric dimer with oxygen atoms of two catechol ligands linking adjacent metal centers. Molybdenum–oxygen lengths within the bridge are quite unsymmetrical with the longest length occurring within the chelate ring to an oxygen which is trans to a strongly bound oxo ligand. The ligands have C–O lengths which are consistent with a fully reduced catechol structure. Accordingly, the metal centers are rare examples of octahedral Mo(VI) having a single oxo ligand. The electronic spectrum of the complex is found to be nearly identical with that of a complex previously characterized as $\text{Mo}(\text{O}_2\text{C}_6\text{H}_2(t\text{-Bu})_2)_3$. A band in the infrared region at 990 cm^{-1} appears attributable to the $\text{Mo}=\text{O}$ stretch and the proton NMR is consistent with the structural result. Electrochemically, the complex is not observed to undergo oxidation but does undergo two irreversible reductions, likely to Mo(V) species.

Introduction

Much of the coordination chemistry of higher oxidation state molybdenum is centered about classes of complexes containing terminal and bridging oxo ligands. Species containing a single oxo ligand, $\text{Mo}=\text{O}^{n+}$, are commonly found in the chemistry of Mo(IV) and Mo(V) but rarely found with Mo(VI).¹ Examples of cases where the MoO^{4+} unit is found include seven-coordinate peroxo and persulfido complexes, $\text{MoO}(\text{X}_2)\text{L}_4^{2+}$ ($\text{X} = \text{O}, \text{S}$),^{2,3} seven-coordinate dithiocarbamate complexes,⁴ $\text{MoO}(\text{dtc})_3^+$, and five-coordinate oxyhalides, MoOX_4 .⁵ We have been interested for some time in complexes prepared with *o*-quinone ligands for their unique magnetic, structural, and electrochemical properties. A convenient route to neutral bis and tris complexes with metals of the first transition series involves simple reaction between the neutral *o*-quinone and an appropriate metal carbonyl. Characterization of complexes formed by this method with metals ranging from vanadium to nickel has indicated that the ligands bond as partially reduced semiquinones (eq 1).^{6–8} While relatively



little has been done with related complexes with second- or third-row metals, reactions carried out with $\text{Mo}(\text{CO})_6$ suggest rather different chemistry. The reaction with tetrachloro-1,2-benzoquinone gave a dimer, $[\text{Mo}(\text{O}_2\text{C}_6\text{Cl}_4)_2]_2$, with fully reduced ligands and Mo(VI) centers.⁹ The same reaction carried out with 9,10-phenanthrenequinone under similar conditions was found to be photochemical and produced the *cis*-dioxomolybdenum(VI) complex $\text{Mo}_2\text{O}_5(\text{O}_2\text{C}_{14}\text{H}_8)_2$ with semiquinone ligands.¹⁰ Razuvaev and co-workers have reported the synthesis of the 3,5-di-*tert*-butylbenzoquinone complex of Mo, $\text{Mo}(\text{O}_2\text{C}_6\text{H}_2(t\text{-Bu})_2)_3$, by the method above and by reaction between MoCl_3 and the semiquinone form of the ligand.¹¹ In view of the interesting structural features of

Table I. Crystal Data for $[\text{MoO}(\text{O}_2\text{C}_6\text{H}_2(t\text{-Bu})_2)_2]_2 \cdot \text{C}_6\text{H}_5\text{CH}_3$

space group $P\bar{1}$	$V = 1595.9 (5) \text{ \AA}^3$
$a = 11.521 (3) \text{ \AA}$	fw 1197.27
$b = 13.125 (3) \text{ \AA}$	$\rho(\text{obsd}) = 1.239 (5) \text{ g cm}^{-3}$
$c = 11.515 (3) \text{ \AA}$	$\rho(\text{calcd}) = 1.242 \text{ g cm}^{-3}$
$\alpha = 108.11 (2)^\circ$	$Z = 1$
$\beta = 97.48 (2)^\circ$	imposed symmetry $\bar{1}$
$\gamma = 100.29 (2)^\circ$	$\mu = 4.42 \text{ cm}^{-1}$

$[\text{Mo}(\text{O}_2\text{C}_6\text{Cl}_4)_2]_2$ and $\text{Mo}(\text{O}_2\text{C}_{14}\text{H}_8)_3$, we have sought to repeat this synthesis but have obtained results from the hexacarbonylmolybdenum–3,5-di-*tert*-butylbenzoquinone reaction which differ considerably from those reported by Razuvaev. Our characterization of the dimeric oxomolybdenum(VI) product obtained from this reaction is the subject of this paper.

Experimental Section

Compound Preparation. The reaction between $\text{Mo}(\text{CO})_6$ and 3,5-di-*tert*-butyl-1,2-benzoquinone was carried out in 50 mL of refluxing toluene by combining 0.53 g (2 mmol) of carbonyl with 1.00 g (6 mmol) of quinone. Over the period of a few hours the solution turned from the dark green color of the quinone to the dark purple color of the complex. It is pertinent to point out that both $[\text{Mo}(\text{O}_2\text{C}_6\text{Cl}_4)_2]_2$ and $\text{Mo}(\text{O}_2\text{C}_{14}\text{H}_8)_3$ are purple while $\text{Mo}_2\text{O}_5(\text{O}_2\text{C}_{14}\text{H}_8)_2$ is green. Other reports have appeared describing the synthesis of "green $\text{Mo}(\text{O}_2\text{C}_{14}\text{H}_8)_3$ " from the reaction of 9,10-phenanthrenequinone and $\text{Mo}(\text{CO})_6$.¹² Initially the reaction was carried out under nitrogen; however, efforts were not made to assure a scrupulously oxygen-free system. The complex must form by reaction with trace quantities of oxygen similar to the 9,10-phenanthrenequinone reaction. The complex itself is air stable and may be isolated from toluene solution as $\text{MoO}(\text{O}_2\text{C}_6\text{H}_2(t\text{-Bu})_2)_2 \cdot \frac{1}{2}\text{C}_6\text{H}_5\text{CH}_3$. The loosely held toluene solvate molecule is easily displaced from the crystal structure at room temperature resulting in decay of crystal quality and erratic chemical analyses for the compound.

Physical Measurements. Infrared spectra were recorded as KBr pellets on a Perkin-Elmer 337 grating spectrophotometer. Visible spectra were recorded on a Cary 17 recording spectrophotometer. A Varian 390 spectrometer was used for NMR spectra. Electrochemical